CELL CYCLE
2018, VOL. 17, NO. 10, 1188–1198
https://doi.org/10.1080/15384101.2018.1467675

Taylor & Francis
Taylor & Francis Group

RESEARCH PAPER

The long non-coding RNA LSINCT5 promotes malignancy in non-small cell lung cancer by stabilizing HMGA2

Yuheng Tian, Nali Zhang, Shuwen Chen, Yuan Ma, and Yanyan Liu

Department of Respiratory, Luoyang Central Hospital, Zhengzhou University, Luoyang, China

ABSTRACT

Long non-coding RNAs (lncRNAs) can actively participate in tumorigenesis in various cancers. However, the involvement of lncRNA long stress induced non-coding transcripts 5 (LSINCT5) in non-small cell lung cancer (NSCLC) remains largely unknown. Here we showed a novel lncRNA signature in NSCLC through lncRNA profiling. Increased LSINCT5 expression positively correlates with malignant clinicopathological features and poor survival. LSINCT5 can promote migration and viability of various NSCLC cells *in vitro* and also enhance lung cancer progression *in vivo*. RNA immunoprecipitation followed by mass spectrometry has identified that LSINCT5 interacts with HMGA2. This physical interaction can increase the stability of HMGA2 by inhibiting proteasome-mediated degradation. Therefore, LSINCT5 may possibly contribute to NSCLC tumorigenesis by stabilizing the oncogenic factor of HMGA2. This novel LSINCT5/HMGA2 axis can modulate lung cancer progression and might be a promising target for pharmacological intervention.

ARTICLE HISTORY
Received 9 November 2017
Accepted 13 April 2018

KEYWORDS
LSINCT5; HMGA2; NSCLC

Introduction

The lung cancer has been a leading cause of cancer-related death especially in China [1] and the non-small cell lung cancer (NSCLC) accounts for over 80% cases with dramatically low five-year survival [2,3]. Therefore, unraveling predictive biomarkers for NSCLC diagnosis as well as identification of efficient therapeutics have been in urgent need.

Although a large portion of human genome is actively transcribed, only around 1% of the genome can encode proteins [4]. The long non-coding RNAs (lncRNAs) denote an important part of transcribed non-coding RNAs with over 200 nucleotides in length [5]. LncRNAs have been shown to be associated with a large array of biological functions including but not restricted to development, epigenetic modulation, apoptosis, chromatin remodeling, autophagy and cell cycle regulation [6–8]. In addition, the profiles of lncRNA expression have been found to be associated with various diseases including cancer [9]. Specifically, numerous studies have demonstrated that lncRNAs are critically involved in lung cancer progression. Recently, Zhang et al. showed that lncRNA HOXA11-AS promotes tumorigenesis in NSCLC through a chick embryo chorioallantoic membrane (CAM) model [10]. Cui et al. showed that SNHG1 promotes NSCLC progression via targeting miR-101-3p and modulates Wnt signaling [11] Instead, TFPI2AS1 may function as a tumor suppressor in NSCLC progression by increasing the expression of cyclin D1 and cyclin-dependent kinases 2 (CDK2) [12]. GAS5 was also identified as a lncRNA with suppressive roles in NSCLC [13]. Various other lncRNAs can also play diverse roles during NSCLC progression [5,14–16]. The long stress induced non-coding transcripts 5 (LSINCT5) is an intergenic lncRNA (5p15.33) which is transcribed from negative strand between IRX4 and IRX2 genes without an open reading frame [17]. However, the potential involvement of LSINCT5 in NSCLC still remains unknown.

In current study, to identify novel lncRNA markers implicated in NSCLC progression, we conducted microarray profiling followed by qRT-PCR analysis. We found that LSINCT5 was consistently upregulated in paired tumor tissues as well as cancerous cell lines (95D cells with high metastatic potential versus 95C cells with low metastasis [18]). The high expression of LSINCT5 is correlated with advanced TNM stages and metastasis. Patients with higher LSINCT5 expression have poor survival. The biological function of LSINCT5 is further verified both in vitro and in vivo. To further explore the oncogenic role of LSINCT5, RNA pulldown followed by mass spectrometry was performed and high mobility group AT-hook 2 (HMGA2) was identified to directly interact with LSINCT5. LSINCT5 can inhibit ubiquitin-mediated HMGA2 degradation and therefore potentially advances NSCLC development. Our current work has identified a novel role of LSINCT5 and implied that LSINCT5 might be an important gene regulator in NSCLC.

Results

Identifying differentially expressed lncRNAs by microarray profiling

The genome-wide lncRNA profiling was performed between paired tumor and adjacent normal tissues and between 95D (with high metastatic potential) and 95C (with low metastatic potential) lung cancer cells [18] to unravel putative cancer-derived or metastasis-related lncRNAs. Two heatmaps were illustrated (Figure 1A and C). The volcano plot was used to show differentially expressed lncRNAs with

CONTACT Yuheng Tian tianyh_lch@yeah.net
Supplemental data for this article can be accessed here.

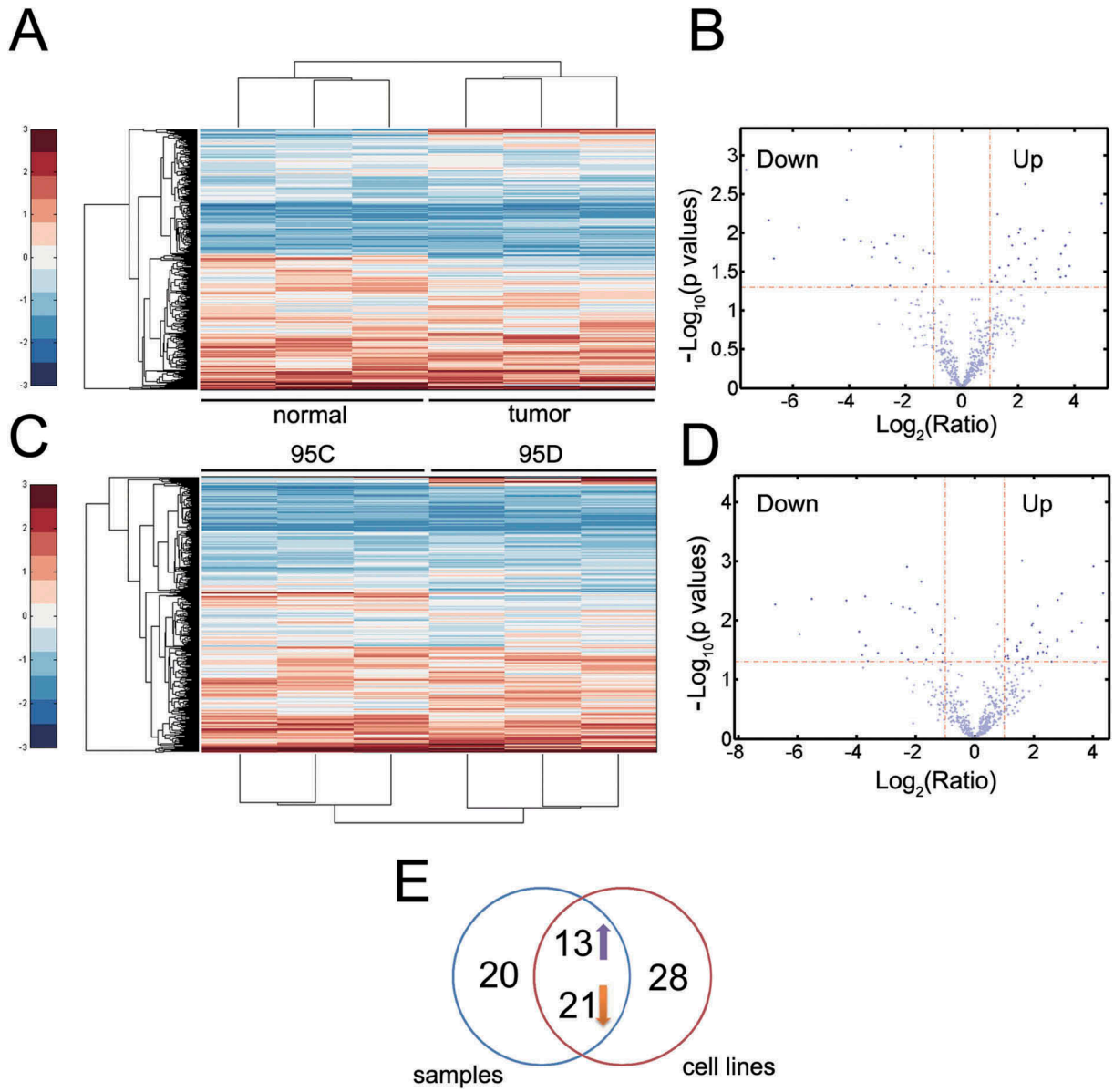

Figure 1. The lncRNA LSINCT5 is associated with malignancy in NSCLC. (A) Heatmap for lncRNA expressions in paired tumor and normal adjacent samples. Samples were shown in columns and lncRNAs were in rows. (B) Volcano plot to filter out significantly expressed lncRNAs for (A). The horizontal red line denotes P = 0.05, while the vertical red curve represents FC = 2. (C) LncRNA profiling for 95C and 95D cells. (B) Volcano plot to identify significantly expressed lncRNAs for (C). (E) Venn diagram indicating consistently upregulated (n = 13) or downregulated (n = 21) lncRNAs in both microarray data.

P < 0.05 and fold change (FC) >2 between the matched groups from the microarray analyses (Figures 1B and D). In paired tumor/normal samples, 54 differentially expressed (i.e. upregulated or downregulated significantly) lncRNAs were identified (Figures 1A and B) while in 95D/95C pairs, 62 differentially expressed lncRNAs were identified (Figures 1C and D). The Venn diagram showed that 34 of the differentially expressed lncRNAs were identified in both sets (paired normal/tumor samples and 95C/95D pair, Figure 1E). Among the 34 dysregulated lncRNAs, 13 lncRNAs were consistently upregulated in both 95D and tumor samples and were therefore regarded as candidate tumor-derived lncRNAs and subjected to subsequent analysis (Figure 1E and Table S1). To identify novel biomarkers, the lncRNAs which have been investigated before were excluded from further study (Table S1). We found that most differentially upregulated lncRNAs have been reported in previous work (Table S1). However, LSINCT5 may represent a novel lncRNA in NSCLC and therefore we chose LSINCT5 for further study.

LSINCT5 is overexpressed in NSCLC tissues with poor survival

To evaluate the clinical significance of LSINCT5, we analyzed the expression of LSINCT5 in 76 paired NSCLC and normal adjacent tissues (Figure 2A). We found that LSINCT5 is significantly upregulated in NSCLC samples (Figure 2A). Moreover, higher LSINCT5 expression correlated with III/IV TNM stages (P < 0.01, Figure 2B). In addition, the metastasis was also positively associated with LSINCT5 expression (Figure 2C). The clinicopathological

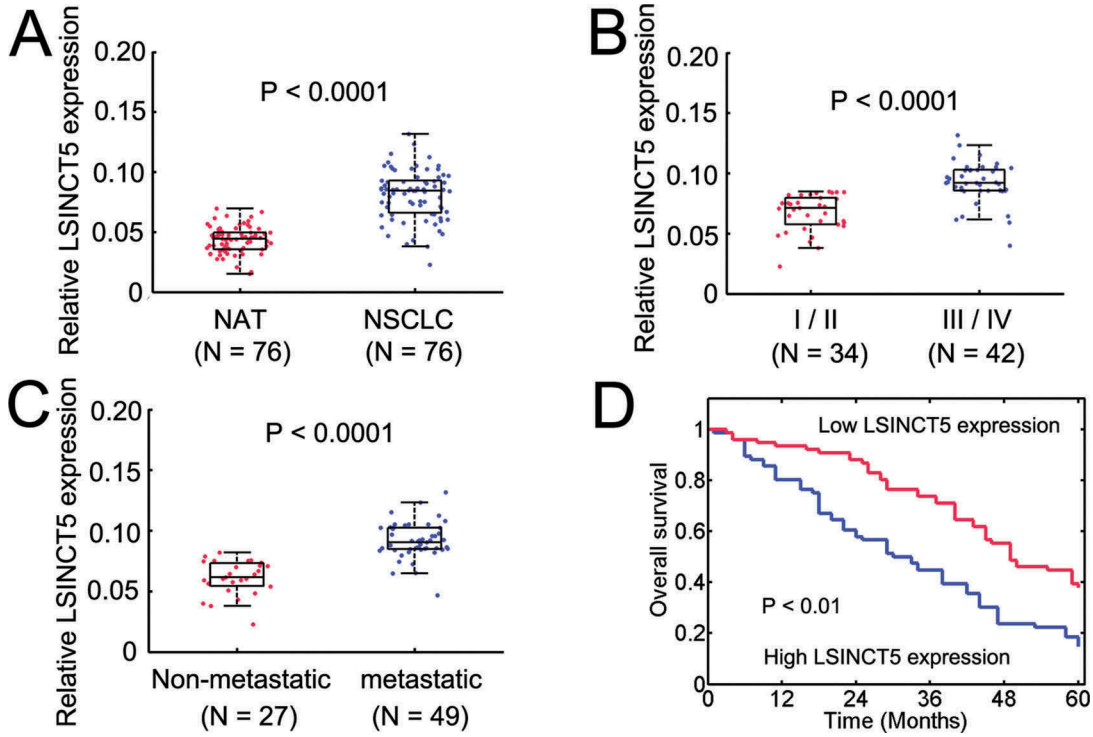

Figure 2. LSINCT5 is overexpressed in NSCLC tissues. (A) The expression of LSINCT5 in 76 NSCLC and pair normal adjacent tissue samples. Expressions were normalized to *GAPDH*. (B and C) Clinical significance for LSINCT5 in NSCLC patients. Higher LSINCT5 expression correlated with TNM stages (III/IV) (B) and metastasis (C). Metastasis denotes lymph node metastasis and/or distal metastasis. (D) Kaplan-Meier survival curves for patients with NSCLC. P < 0.01 by log-rank test.

features of enrolled patients were listed in Table 1. We found that LSINCT5 was not correlated with age, gender and histological subtypes (Table 1). However, tumor size, TNM stages and metastasis were significantly affected by LSINCT5 expression (Table 1). Furthermore, higher LSINCT5 expression substantially correlated with poor outcomes in NSCLC patients (Figure 2D). These results suggested that LSINCT5 is overexpressed in NSCLC and predicts poor prognosis.

Table 1. Correlation between clinicopathological parameters and tumorous LSINCT5 expression (N = 76).

Clinicopathological parameters	Patient number	LSINCT5 expression Low (N = 38) (N, %)	LSINCT5 expression High (N = 38) (N, %)	*P* values
Age				
< 60	43	23 (53.5%)	20 (46.5%)	0.322
≥ 60	33	15 (45.5%)	18 (54.5%)	
Gender				
Male	46	26 (56.5%)	20 (43.5%)	0.120
Female	30	12 (40.0%)	18 (60.0%)	
TNM Stage				
I/II	34	24 (70.6%)	10 (29.4%)	0.002*
III/IV	42	14 (33.3%)	28 (66.7%)	
Tumor Size				
< 4 cm	25	19 (76.0%)	6 (24.0%)	0.003*
≥ 4 cm	51	19 (37.3%)	32 (62.7%)	
Metastasis				
Negative	27	20 (74.1%)	7 (25.9%)	0.004*
Positive	49	18 (36.7%)	31 (63.3%)	
Histological subtype				
Squamous cell carcinoma	40	18 (45.0%)	22 (55.0%)	0.245
Adenocarcinoma	36	20 (55.6%)	16 (44.4%)	

Abbreviations: TNM, tumor (T), the extent of spread to the lymph nodes (N), and the presence of metastasis (M). (* $P < 0.05$)

LSINCT5 promotes NSCLC cell growth

We have established a relation between LSINCT5 and poor outcomes in NSCLC patients, we next explored whether LSINCT5 had oncogenic potentials *in vitro*. We evaluated the expression of LSINCT5 in various lung cancer cell lines and found that LSINCT5 was overexpressed in cancerous cells compared with the normal control (Fig. S1). LSINCT5 overexpression significantly enhanced migration of 95C cells (P < 0.01, Figure 3A and Fig. S2A). Meanwhile, si-RNA mediated LSINCT5 knockdown significantly lowered the migration in 95D cells (P < 0.01, Figure 3B and Fig. S2B, si-LSINCT5 #2 was used if not otherwise specified). Qualitatively similar results can be obtained from LSINCT5-overexpressing H838 cells (Figure 3C) and si-LSINCT5 A549 cells (Figure 3D). We further investigated the viability of NSCLC cells by altering LSINCT5 expression. We found that 95C cells with LSINCT5-overexpression markedly increased the viability (Figure 3E). Furthermore, lowering LSINCT5 levels in 95D cells substantially attenuated the viability (Figure 3F). In H838 and A549 cells, qualitatively similar results can be observed (Figure 3G and H). These results suggested that LSINCT5 enhanced NSCLC progression *in vitro*.

Xenograft model identifies oncogenic role of LSINCT5

To further confirm the role of LSINCT5 *in vivo*, we conducted xenograft mouse model (For model selection, please refer to materials and methods). We found that the tumor volume of 95D cell xenografts was substantially reduced with LSINCT5 knockdown (Figure 4A, P < 0.01). In addition, the tumor weight was also markedly decreased with shLSINCT5 in 95D

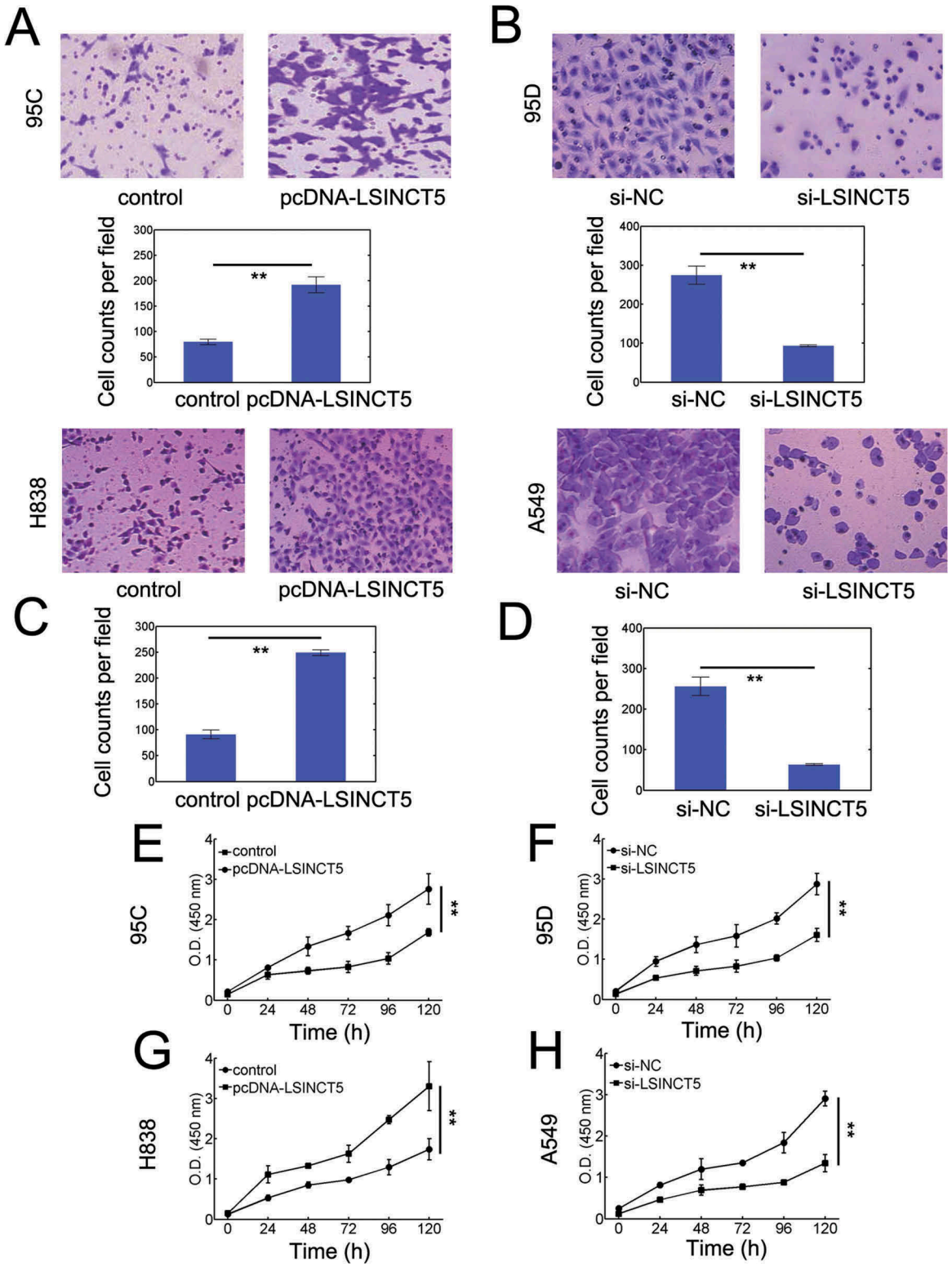

Figure 3. LSINCT5 advances migration and viability *in vitro*. (A) Transwell migration assay for 95C cells transfected with either pcDNA3.1 (pcDNA) or pcDNA-LSINCT5. (B) Transwell migration assay for 95D cells transfected with either si-NC or si-LSINCT5. (C) Transwell migration assay for H838 cells transfected with either pcDNA3.1 (pcDNA) or pcDNA-LSINCT5. (D) Transwell migration assay for A549 cells transfected with either si-NC or si-LSINCT5. Quantification results were shown at bottom in panels (A-D). **: $P < 0.01$. CCK-8 viability assays for 95C (E), 95D (F), H838 (G) and A549 (H) cells. **: $P < 0.01$. 95C and H838 cells were transfected with either pcDNA or pcDNA-*LSINCT5*. 95D and A549 cells were treated with either si-NC or si-LSINCT5 as indicated.

xenograft models (Figure 4C). Consistently, tumor growth in 95C cell xenografts was significantly increased with LSINCT5 overexpression (Figure 4B, $P < 0.01$) leading to higher tumor weights (Figure 4D). There was evidence of metastatic nodules in 95D shCtrl group (see arrows, Figure 4E, top). However, the metastatic nodules were absent or substantially reduced with LSINCT5 knockdown (Figure 4E and F, top). Not surprisingly, LSINCT5 overexpression markedly

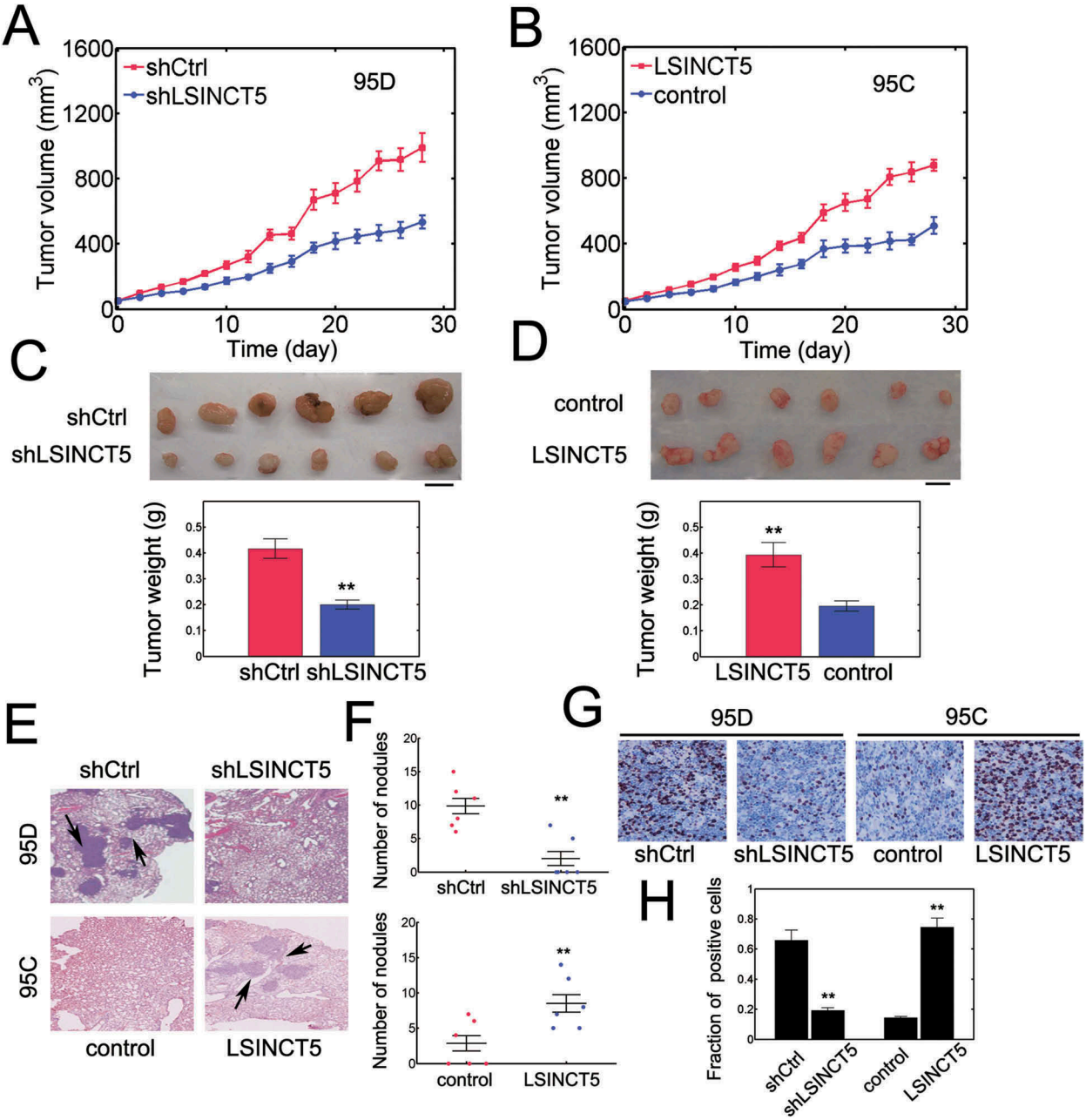

Figure 4. LSINCT5 promotes NSCLC progression in *vivo*. (A) Tumor volume was quantified every 2 days for 28 days in 95D cell xenograft mouse model. 95D cells were either transfected with pLKO1-shRNA-control (shCtrl) or pLKO1-sh-LSINCT5 (shLSINCT5). **: P < 0.01. (B) Tumor volume was quantified in 95C cell xenograft mouse model. 95C cells were either transfected with pWPXL-Vec (control) or pWPXL-LSINCT5 (LSINCT5). **: P < 0.01. (C) By the end of implantation, solid tumors were resected and weighted in either 95D shCtrl or shLSINCT5 xenograft tumors. Representative images were shown (top). Tumor weight was evaluated (bottom). **: P < 0.01. (D) Tumor weight was measured in either 95C pWPXL-Vec (control) or pWPXL-LSINCT5 (LSINCT5) xenograft tumors. Representative images were shown (top). Tumor weight was evaluated (bottom). **: P < 0.01. (E) H&E staining for lung sections. **: P < 0.01. ×100 magnification. (F) The number of metastatic nodules in lung sections was quantified. (G) Ki-67 staining for tumor slides. (H) Quantification of Ki-67 positive fractions. **: P < 0.01.

increased the number of metastatic nodules in 95C xenografts (Figure 4E and F, bottom). Ki-67 staining also confirmed that shLSINCT5 greatly obviated the proliferation of NSCLC xenograft tumors while LSINCT5 overexpression potentiated tumor growth (Figure 4G and H). These results suggested that LSINCT5 also plays an oncogenic role *in vivo*.

LSINCT5 interacts with HMGA2 in NSCLC cells

To further identify the potential mechanisms of LSINCT5 mediated tumor promotion, we performed LSINCT5 pulldown followed by mass spectrometry. The results showed a specific band at ~50 kD (Figure 5A). This band was resected and subject to mass spectrometry. The results identified 8 putative proteins (Table S2). Immunoblots further confirmed that HMGA2 interact physically with LSINCT5 (Figure 5B). RIP experiments also showed that LSINCT5 enrichment was dramatically elevated in pulldown with primary antibody against HMGA2 (Figure 5C). To further identify the binding regions of LSINCT5 with HMGA2, we constructed various LSINCT5 mutants (Table S3, Figure 5D and S3A). The results showed that the 1–602 nt fragment was responsible for its

association with HMGA2 (Figure 5E). On the other hand, serial HMGA2 depletion mutants were constructed to map the interacting regions which are required for the LSINCT5-HMGA2 complex (Table S4, Figure 5F and S3B). HMGA2 contains three AT-hook domains (green regions, Figure 5F, left) and an acidic C-terminal tail (orange region, Figure 5F, left). [19] We found that the second AT-hook domain was responsible for HMGA2 binding to LSINCT5 (Figure 5F, right). Δ42-70 mutant with the depletion at the second AT-hook failed to bind LSINCT5 (Figure 5F, right). These results suggested that LSINCT5 physically interacts with HMGA2 in NSCLC cells.

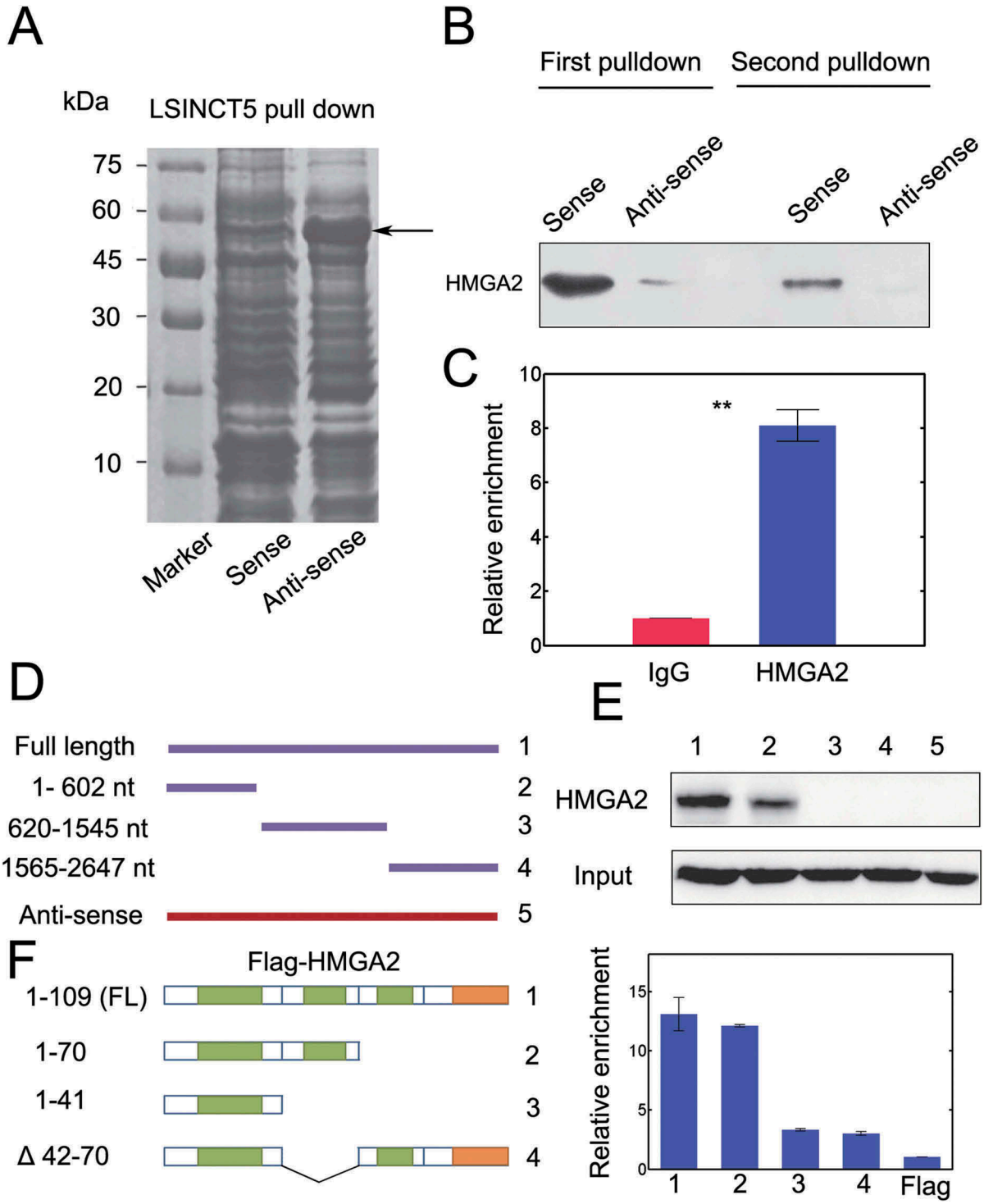

Figure 5. LSINCT5 interacted with HMGA2 in NSCLC cells. (A) Biotin labeled LSINCT5-sense and LSINCT5 anti-sense probes were transcribed in vitro and incubated together with 95D lysates. The ~50 kD band was (arrows) excised and subject to mass spectrometry analysis. (B) Immunoblots for interaction between LSINCT5 and HMGA2 from two independent RNA pull-down assays. (C) RIP assays were done using primary antibody against HMGA2 and qPCR was used to identify LSINCT5. (D) Illustration of different truncated forms, full length (FL) and anti-sense probe of LSINCT5. (E) Immunoblots for LSINCT5 pull-down with HMGA2 using full-length (FL), various truncated forms and anti-sense probe. (F) Identification of interaction domains of HMGA2 with LSINCT5. RIP assays for LSINCT5 enrichment in 95D cells transfected with FL or different truncated forms of HMGA2. Enrichment quantification was shown on the right.

LSINCT5 interacts with HMGA2 to inhibit its proteasome-mediated degradation

We next investigated the potential function of the interaction between LSINCT5 and HMGA2. We quantified *HMGA2* mRNA expression under various conditions and found that LSINCT5 had no impact on *HMGA2* mRNA levels (Figure 6A). However, we indeed found that LSINCT5 increased the protein abundance of HMGA2 (Figure 6B). The protein stability of HMGA2 was markedly damped by si-LSINCT5 (Figure 6C). Moreover, the protein degradation was inhibited after treatment of the proteasome inhibitor MG132 (Figure 6C) implying that LSINCT5 can suppress proteasome-mediated degradation of HMGA2. Similar results can be found in A549 cells (Figure 6D). The ubiquitination of HMGA2, as expected, was substantially elevated with si-LSINCT5 and was suppressed with LSINCT5 overexpression (Figure 6E). The migratory capacity of NSCLC cells was dramatically attenuated when HMGA2 was silenced (Figure 6F and S2C). Consistently, LSINCT5 overexpression additionally increased the migration while si-HMGA2 counteracted this effect (Figure 6F). Notably, the siRNA or overexpression efficiency was verified (Fig. S2C and S2D, si-HMGA2 #2 showed higher efficiency and was selected as si-HMGA2 thereafter). Furthermore, HMGA2 overexpression can rescue the effect of deficiency in LSINCT5 and increased the migration (Figure 6G). LSINCT5 knockdown then reversed the effect of HMGA2 overexpression (Figure 6G). These results suggested that LSINCT5 physically interacts with HMGA2 to protect HMGA2 from proteasome-mediated degradation.

Discussion

The discovery of lncRNAs has helped us elucidate the underlying mechanisms of oncogenesis and provided novel clues by serving as diagnostic markers [20]. Owing to its readily accessibility such as in plasma, urine and serum [21,22], lncRNAs has advantages to be employed as biomarkers. Since lung cancer represents a leading cause of mortality in tumor-related death, unraveling effective and predictive biomarkers may help early diagnosis and improve survival of lung cancer patients. Through microarray profiling, we have identified novel lncRNA signatures related to NSCLC progression. Especially, the lncRNA LSINCT5 may function as an oncogenic lncRNA at least in NSCLC. As a result, identification of LSINCT5 may advance our understanding of the molecular processes implicated in lung cancer metastasis.

In current study, we have demonstrated an increased expression pattern of LSINCT5 at least in NSCLC tissues and cell lines (Figures 1 and 2). LSINCT5 is critically associated with advanced TNM stages and tumor growth (Figure 1 and Table 1). Migration and viability assays confirmed the oncogenic role of LSINCT5 *in vitro*, with attenuated malignancy when LSINCT5 was knocked down (Figure 3). Furthermore, the *in vivo* xenograft mouse model again shed light on the pivotal role of LSINCT5 to promote NSCLC development (Figure 4). RIP followed by mass spectrometry identified HMGA2 as a direct target of LSINCT5 (Figure 5). LSINCT5 can interact with HMGA2 to block its degradation by proteasome to accelerate NSCLC cell migration (Figure 6). These results collectively suggest that LSINCT5 behaves as an oncogenic factor in NSCLC progression.

The high mobility group A (HMGA) proteins are architectural transcription factors and may help the assembly of protein complexes during gene expression. [19] One member in this family is HMGA2, which is ubiquitously expressed during embryogenesis with high expression level and becomes even undetectable in adult tissues [19,23]. However, during neoplasms, HMGA2 can be dramatically upregulated and contributes largely to tumor cell growth and proliferation [24]. Previous findings have shown that HMGA2 might result in accumulation of genomic instabilities and therefore actively contribute to various cancers [25,26]. Reactivation of *HMGA2* expression is usually mediated through chromosomal translocation in malign tumors [27]. Overexpression of *HMGA2* has been shown in various malignant tumors such as NSCLC, pancreatic cancer, breast cancer, endometrial carcinoma, squamous cell carcinoma and leukemia [17,24,28–30]. Especially, HMGA2 protein levels positively correlated with advanced tumor grade in a wide array of lung cancers [31]. HMGA2 is also required for transformation in many NSCLC cells [31]. Overexpressing HMGA2 also induces epithelial-mesenchymal transition (EMT), which has been implicated in metastatic phenotypes in tumor cells [32]. Therefore, HMGA2 may be causally involved in neoplasm. Taken together, HMGA2 might function as a general marker for carcinogenesis for various tumor types.

Our study showed that LSINCT5 physically interact with HMGA2 and significantly increases its stability (Figures 5 and 6). Overexpressing HMGA2 can counteract the effect of si-LSINCT5 in NSCLC cells to promote migration. Therefore, we argue that LSINCT5 may fulfill its oncogenic role at least in part by stabilizing HMGA2. Since HMGA2, as demonstrated above, can serve as an oncogenic indicator in numerous cancers, stabilization of HMGA2 via LSINCT5 may greatly advance NSCLC progression via diverse mechanisms [31,33].

There might be alternative strategies used by LSINCT5 for NSCLC progression. For instance, recent evidence has suggested that lncRNAs may function as competitive endogenous RNAs (ceRNAs) and regulate tumorigenesis [34,35]. For example, HOXD-AS1 competitively binds miR-147a to promote NSCLC development [34]. LncRNA GAS5, however, may increase radio-sensitivity in NSCLC cells by suppressing miR-135 [35]. Searching for potential ceRNAs for LSINCT5 involved in NSCLC progression may present a promising clue for NSCLC diagnosis and deserve in-depth investigation in future.

In conclusion, our current work has revealed that lncRNA LSINCT5 serves as a novel oncogenic factor which is critically involved in NSCLC progression. LSINCT5 can enhance malignant phenotypes of lung cancer both *in vitro* and *in vivo*. LSINCT5 contributes to NSCLC tumorigenesis partially by physical interaction with and stabilizing HMGA2. This novel identified LSINCT5/HMGA2 axis may represent a promising target for pharmacological intervention.

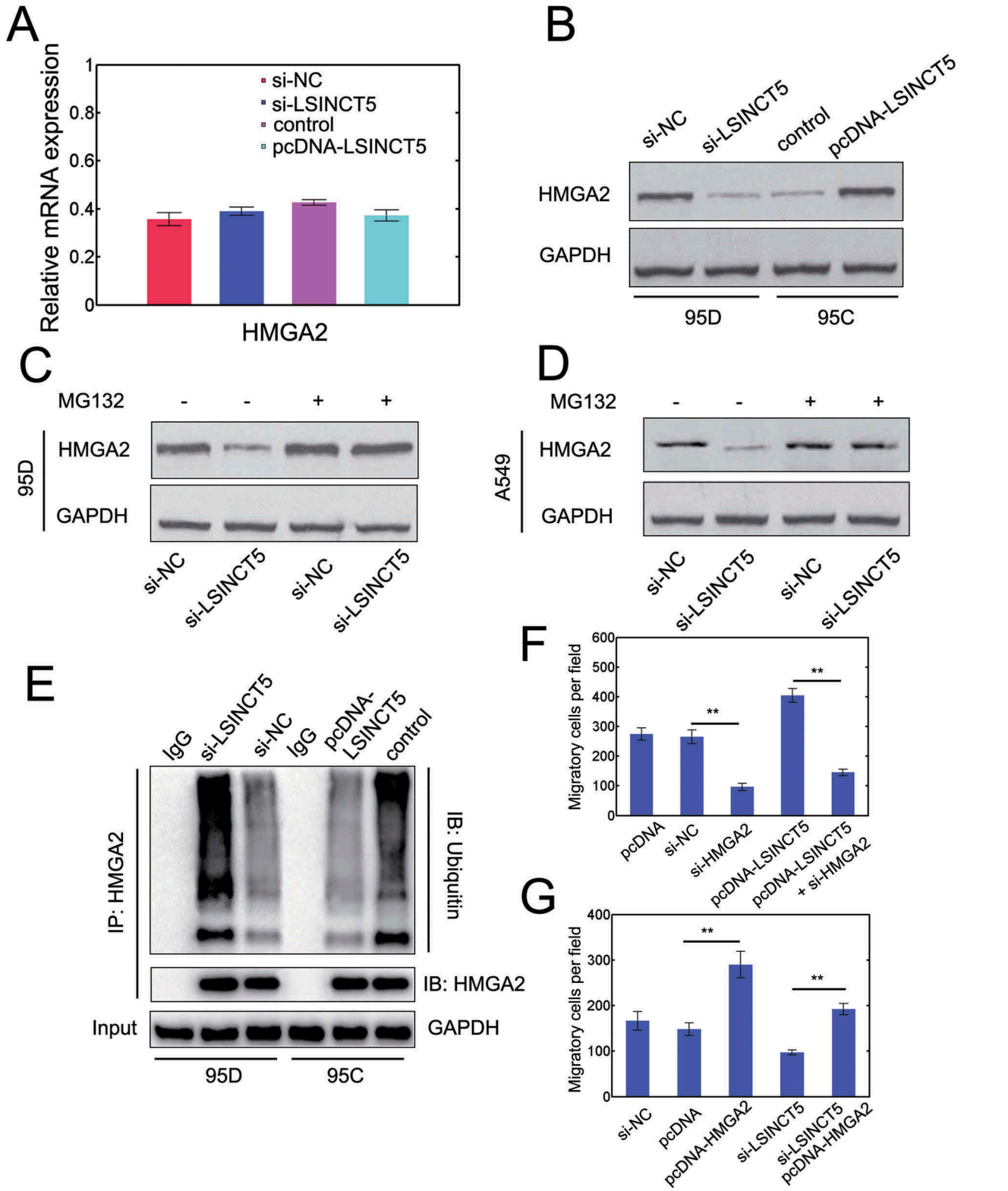

Figure 6. LSINCT5 physically interacts with HMGA2 to inhibit its degradation. (A) Relative *HMGA2* mRNA levels with si-LSINCT5 transfection in 95D cells or pcDNA-LSINCT5 transfection in 95C cells. (B) Immunoblots for HMGA2 protein expression by si-LSINCT5 in 95D cells or pcDNA-LSINCT5 transfection in 95C cells. (C) 95D cells were transfected with si-NC or si-LSINCT5 and then treated with MG132 (30 μM) for 12 h followed by immunoblot for HMGA2. (D) A549 cells were transfected with si-NC or si-LSINCT5 and then treated with MG132 (30 μM) for 12 h followed by immunoblot for HMGA2. (E) Cell lysates from 95D cells with si-LSINCT5 or 95C cells with LSINCT5 overexpression were immunoprecipitated with HMGA2 and then subject to immunoblot towards ubiquitin or HMGA2. (F) Migration in 95D cells transfected with pcDNA, si-NC, si-*HMGA2* (#2), pcDNA-LSINCT5 or pcDNA-LSINCT5 plus si-HMGA2. **: $P < 0.01$. (G) Rescue transwell migration assays were done in 95C cells. LSINCT5 were silenced or not and 95C cells were transfected with either pcDNA or pcDNA-*HMGA2*. **: $P < 0.01$.

Materials and methods

Cell lines and reagents

All the lung cancer cell lines (WI-38, A549, H1299, 95D, 95C and H838) were obtained from Shanghai Institute of Biochemistry and Cell Biology. All cell lines were maintained in humidified atmosphere with 5% CO_2 in Dulbecco's Modified Eagle Media (DMEM, no.D5796, Sigma, Shanghai, China) plus 5% fetal bovine serum (FBS, no.F8067, Sigma, Shanghai, China) and 100 μg/ml streptomycin (no.V900929, Sigma, Shanghai, China). Antibodies against GAPDH (no.8795) and HMGA2 (no.WH0008091M1) were purchased from Sigma (Shanghai, China). The proteasome inhibitor MG132 was obtained from Sigma (no.M8699, Shanghai, China).

Human samples

The human NSCLC samples (N = 76) and corresponding normal adjacent tissues (at least 3 cm away from tumors) were obtained from Luoyang Central Hospital between January 2011 and May 2012. The specimens were stored at −80°C refrigerator before analysis. None patients have received preoperative chemotherapy or radiotherapy. The experimental protocols were approved by the Ethical Review Committee of the Luoyang Central Hospital. Informed consent was obtained from all patients.

RNA extraction and quantitative real-time RT-PCR (qRT-PCR)

Total RNAs were extracted using the TRIzol reagents (Invitrogen) according to the manufacturer's instructions. The quantification of RNA was performed using Nanodrop 2000 (Thermo Scientific, Shanghai, China). The cDNA was synthesized using PrimeScript RT Reagent Kit (TaKaRa, Shanghai, China). The qRT-PCR was performed with SYBR Green Premix Ex Taq (TaKaRa, Shanghai, China). Reactions were performed with ABI PRISM® 7000 Sequence Detection System (Applied Biosystem, USA) according to the manufacturer's instructions. The primers were listed as follows: LSINCT5, forward: GTAGCGTCTGATT, reverse: TC GCGATCTCGT; *HMGA2*, forward: TATGGTGTGGACATA, reverse: ATGCGCTTAGGTTC; *GAPDH*, forward: ATAGAGTC GAAGCTCTTATC, reverse: CGCAGATCGTCTGCGATCAGA.

RNA interference

The small interfering RNAs (siRNAs) specific for LSINCT5 and *HMGA2* as well as the siRNA negative controls (si-NCs) were designed and synthesized by GenePharma (Shanghai, China). The cells were transfected with indicated siRNAs using Lipofectamine 2000 (Invitrogen, CA, USA) for 48 hours according to the manufacturer's protocols. The sequences for siRNA were provided below: si-LSINCT5#1: 5′-GAACTGGATTAGTGTTAAATT-3′

si-LSINCT5#2: 5′-TTCAGAGGTTTGTAGCTGGTT-3′

si-HMGA2#1: 5′-AACGGCCAAGAGGCAGACCTA-3′

si-HMGA2#2: 5′-CAGCGGCGGCAGCCTAAGCAA-3′

Vector construction

The expression vector pcDNA3.1 together with LSINCT5 and *HMGA2* fragments was digested using *Xho*I and *BamHI*. Target genes and pcDNA3.1 were incubated together for 24 h at 4°C with a ratio 10:1. The next day, pcDNA-*LSINCT5* and pcDNA-*HMGA2* recombinant plasmids were harvested and transformed into *E.coli* for 12 h at 37°C. After the incubation, colonies were selected randomly and cultivated at LB medium containing ampicillin. Transfection into cells was performed with Lipofectamine 2000 (Invitrogen, CA, USA) according to the manufacturer's protocols.

Viability assay

We used the Cell Counting Kit-8 (CCK-8, Dojindo, Kumamoto, Japan) to analyze the viability. After treatment for 24 hours, cells were re-suspended and loaded into a 24-well plate (~10^5 cells/well) and for 5 days. A total 10 μl CCK-8 solutions were added into culture. The crystalline formazan was resolved in 100 μL sodium dodecyl sulfate (SDS, 10%, Sigma, Shanghai, China) solution for 24 hours. The optical density was detected at the wavelength of 450 nm using the Spectramax M5 microplate monitor according to the manufacturer's protocol (Molecular Devices LLC, Sunnyvale, CA, USA).

Transwell migration assay

The migration assays were performed using the 24-well transwell chambers (8 μm pore size; BD Biosciences, San Jose, CA, USA). About 1×10^5 cells per well were seeded into the upper chambers. DMEM (500 μl) containing 5% FBS was added into bottom chambers. Cells were suspended in DMEM (200 μl) without FBS. After 24 h's incubation at 37°C, those cells which did not migrate into the lower chambers were removed and cells moved onto the lower chambers were stained with crystal violet (0.2%) for 15 min. The CKX41 inverted microscope was used to visualize the results (Olympus, Japan).

The RNA pulldown and mass spectrometry

The biotin-labelled LSINCT5 was synthesized with the Biotin RNA Labeling Mix by T7 RNA polymerase followed by incubation with cell lysates for 3 h. The biotin-labelled LSINCT5 together with putative interacting proteins were pulled down using streptavidin magnetic beads (Invitrogen, Shanghai, China). Cells were pre-incubated overnight before RNA pulldown. Electrophoresis was used to separate the samples and specific bands were investigated using mass spectrometry (MS). Mass spectrometry was performed in National Laboratory of Protein Engineering and Plant Genetic Engineering of Peking University. The primers were: sense: forward: CGAGGCTAGGGGGCTAGTGCAGTTA; reverse: TGC TGCCAAGTACGCTATT; anti-sense: forward: GCAAATTCC ATCT; reverse: TACGACTCACTATATACTGCAACTCCCTT CCAAG.

RNA immunoprecipitation

The RNA immunoprecipitation (RIP) was performed using the Imprint® RNA Immunoprecipitation Kit (Sigma, Shanghai, China) according to the manufacturer's instructions. Total RNAs and those precipitated with IgG were simultaneously evaluated. 10 μg HMGA2 antibodies were used at the supernatant. Precipitated RNAs were separated using the protein G beads and then quantified with q-PCR.

LncRNA microarray

The lncRNA human Gene Expression Microarray (CapitalBiol, Beijing, China) was used. Briefly, cDNAs containing a T7 RNA polymerase promoter were synthesized from 400 ng RNAs with reverse transcriptase according to the manufacturer's protocols. The DNA products were then purified using NucleoSpin® Extract II kit (Macherey-Nagel, Germany) followed by elution with 20 μl elution buffer. The complementary RNAs were the DNA products using T7 Enzyme Mix for 12 h and subject to purification with NucleoSpin® RNA clean-up kit (Macherey-Nagel, Germany). The amplified RNA (5 μg) was first mixed with 2 μg random primer, denatured at 70°C for 10 min and cooled down. Then, 1 μl 0.2M DTT, 4 μl first-strand buffer and 2 μl reverse CbcScript II transcriptase was used. The whole system was maintained at room temperature for 20 min. The cDNAs were purified using NucleoSpin® Extract II kit (Macherey-Nagel, Germany) and then mixed with 2 μg random primer and heated to 95°C for 2 min followed by cooling down on ice. Furthermore, 10 μl Klenow buffer, dNTP and Cy5(or Cy3)-dCTP were appended leading to 300 M dATP, dTTP, dGTP, 150 M dCTP together with 50 M Cy-dCTP. Reactions were done at 37°Cfor 100 min. The labeled cDNA was purified using NucleoSpin® Extract II kit (Macherey-Nagel, Germany). The array hybridization was performed in CapitalBiol. Finally, the slides were scanned on Agilent microarray scanner. The intensity values were represented using Feature Extraction Software (Agilent Technologies, CA, USA) followed by quartile normalization. Fold change (FC) >2 and $P < 0.05$ was used as the selection criteria. Hierarchical clustering was done using MATLAB (The MathWorks, Inc).

Lentiviral transduction

Lentiviral vector and packaging vectors were transfected into 293T cells. The medium was changed after transfection for 12 h, and the medium containing lentivirus was collected after 36h. All lentiviral vectors (pLKO1-shRNA-control, pLKO1-sh-LSINCT5, pWPXL-Vec and pWPXL-LSINCT5, efficiencies were verified in Figure S4) were designed, synthesized and purchased from Sigma (Mission shRNA library). Transfection was performed with Lipofectamine 2000 (Invitrogen). The shLSINCT5#2 showed higher efficiency and was selected (i.e. shLSINCT5 thereafter, Fig. S4 and Table S5).

Western blot

The cell lysates were extracted with RIPA lysis buffer with protease inhibitors (no.R0278, Sigma, Shanghai, China) and cleared by centrifugation (10,000 g) at 4°C for 20 min. The protein samples were subject to separation using 6% sodium dodecyl sulfate (SDS)-PAGE and transferred to nitrocellulose filter membranes (Millipore, USA). By blocking using PBST containing 4% nonfat milk, all membranes were incubated with primary antibodies.

Xenograft mouse model

95D cells transfected with either pLKO1-shRNA-control (shCtrl) or pLKO1-sh-LSINCT5 (shLSINCT5) or 95C cells transfected with pWPXL-Vec (control) or pWPXL-LSINCT5 (LSINCT5) were maintained in DMEM as described for additional 24 hours. Since LSINCT5 was highly expressed in 95D cells and showed relatively low expression in 95C cells (Fig. S1), we only knocked down LSINCT5 in 95D cells while overexpressed LSINCT5 in 95C cells. Then, cells were resuspended and ~10^6 cells were injected subcutaneously into the flanks (for xenograft tumor growth) or injected into the lateral tail veins of nude mice (for metastatic assays). Tumor growth was monitored every two days. Tumor volume was evaluated by ellipsoid formula: $1/2*D*d^2$, where 'D' denotes the longest diameter while 'd' represents the smallest diameter of solid tumors [36]. Totally, BALB/C nude mice (female, 5 ~ 6 weeks old, n = 6 for each group) were used in current study and obtained from the Model Animal Research Center (Nanjing, China). All animals were housed at 20 ~ 22°C at a 12/12 light/dark cycle with access to food and water *Ad libitum*. Animal experimental protocols and care were in accordance with guidelines and approved by the Animal Use and Care Committee of the Luoyang Central Hospital. By the end of the experiments, animals were sacrificed by overdose of pentobarbital. Tumors were resected and weighted. The lung tissues were fixed in PB-buffered formalin. Then, fixed specimens were loaded in paraffin using the Microm Tissue Embedding Center (Labequip, Ltd.) followed by staining with hematoxylin and eosin (H&E). Ki-67 staining was performed with a Ki-67 ELISA kit (no.MBS930876, MyBioSource, CA, USA).

Immunohistochemistry

The staining was performed with deparaffinized sections as previously described [37] In brief, 5 μm sections were cut down and hydrated sections were blocked by 3% H_2O_2 in water for 10 min. The 10 mmol/L citrate buffer (pH 6.0, for 10 min) was used for antigen retrieval and a cooldown was completed through washing in TBST. Slides were blocking agent (Biocare Medical, Concord, CA) to exclude nonspecific binding. Then, various primary antibodies were incubated with slides for 30 min and then washed in TTBS twice. Finally, slides were incubated with 3,3′-diaminobenzidine (no.D8001, Sigma, Shanghai, China) and counterstained by hematoxylin.

Statistical analysis

Data were represented as mean±SD from at least three experiments. The student's t test was used to identify the statistical significance between two groups while one-way ANOVA was

performed for comparison among multiple groups. The log-rank test was used to evaluate the survival. $P < 0.05$ was considered statistically significant. Analysis was performed using the SPSS software (version 16.0, SPSS Inc., Chicago, IL, USA).

Disclosure statement

No potential conflict of interest was reported by the authors.

References

1. Chen W, Zheng R, Baade PD, et al. Cancer statistics in China, 2015. CA Cancer J Clin. 2016;66:115–132.
2. Tian H, Zhou C, Yang J, et al. Long and short noncoding RNAs in lung cancer precision medicine: opportunities and challenges. Tumour Biol. 2017;39:1010428317697578.
3. Goldstraw P, Ball D, Jett JR, et al. Non-small-cell lung cancer. Lancet. 2011;378:1727–1740.
4. Djebali S, Davis CA, Merkel A, et al. Landscape of transcription in human cells. Nature. 2012;489:101–108.
5. Ricciuti B, Mencaroni C, Paglialunga L, et al. Long noncoding RNAs: new insights into non-small cell lung cancer biology, diagnosis and therapy. Med Oncol. 2016;33:18.
6. Wang K, Liu CY, Zhou LY, et al. APF lncRNA regulates autophagy and myocardial infarction by targeting miR-188-3p. Nat Commun. 2015;6:6779.
7. Peng Z, Zhang C, Duan C. Functions and mechanisms of long noncoding RNAs in lung cancer. Onco Targets Ther. 2016;9:4411–4424.
8. Wang R, Shi Y, Chen L, et al. The ratio of FoxA1 to FoxA2 in lung adenocarcinoma is regulated by LncRNA HOTAIR and chromatin remodeling factor LSH. Sci Rep. 2015;5:17826.
9. Kunej T, Obsteter J, Pogacar Z, et al. The decalog of long noncoding RNA involvement in cancer diagnosis and monitoring. Crit Rev Clin Lab Sci. 2014;51:344–357.
10. Zhang Y, Chen WJ, Gan TQ, et al. Clinical significance and effect of lncRNA HOXA11-AS in NSCLC: a study based on bioinformatics, in vitro and in vivo verification. Sci Rep. 2017;7:5567.
11. Cui Y, Zhang F, Zhu C, et al. Upregulated lncRNA SNHG1 contributes to progression of non-small cell lung cancer through inhibition of miR-101-3p and activation of Wnt/beta-catenin signaling pathway. Oncotarget. 2017;8:17785–17794.
12. Gao S, Lin Z, Li C, et al. TFPI2AS1, a novel lncRNA that inhibits cell proliferation and migration in lung cancer. Cell Cycle. 2017;16:1–10.
13. Xue Y, Ni T, Jiang Y, et al. Long noncoding RNA GAS5 inhibits tumorigenesis and enhances radiosensitivity by suppressing miR-135b expression in non-small cell lung cancer. Oncol Res. 2017;25:1305–1316.
14. Dong Y, Huo X, Sun R, et al. LncRNA Gm15290 promotes cell proliferation and invasion in non-small cell lung cancer through directly interacting with and suppressing the tumor suppressor miR-615-5p. Oncol Res. 2017. DOI:10.3727/096504017X14930316817366
15. Wang L, Chen Z, An L, et al. Analysis of long non-coding RNA expression profiles in non-small cell lung cancer. Cell Physiol Biochem. 2016;38:2389–2400.
16. Yang J, Lin J, Liu T, et al. Analysis of lncRNA expression profiles in non-small cell lung cancers (NSCLC) and their clinical subtypes. Lung Cancer. 2014;85:110–115.
17. Silva JM, Boczek NJ, Berres MW, et al. LSINCT5 is over expressed in breast and ovarian cancer and affects cellular proliferation. RNA Biol. 2011;8:496–505.
18. Zequn N, Xuemei Z, Wei L, et al. The role and potential mechanisms of LncRNA-TATDN1 on metastasis and invasion of non-small cell lung cancer. Oncotarget. 2016;7:18219–18228.
19. Fedele M, Visone R, De Martino I, et al. HMGA2 induces pituitary tumorigenesis by enhancing E2F1 activity. Cancer Cell. 2006;9:459–471.
20. Roth A, Diederichs S. Long noncoding RNAs in lung cancer. Curr Top Microbiol Immunol. 2016;394:57–110.
21. Dong L, Qi P, Xu MD, et al. Circulating CUDR, LSINCT-5 and PTENP1 long noncoding RNAs in sera distinguish patients with gastric cancer from healthy controls. Int J Cancer. 2015;137:1128–1135.
22. Schmitt AM, Chang HY. Long noncoding RNAs in cancer pathways. Cancer Cell. 2016;29:452–463.
23. Chiappetta G, Avantaggiato V, Visconti R, et al. High level expression of the HMGI (Y) gene during embryonic development. Oncogene. 1996;13:2439–2446.
24. Meyer B, Loeschke S, Schultze A, et al. HMGA2 overexpression in non-small cell lung cancer. Mol Carcinog. 2007;46:503–511.
25. Boo LM, Lin HH, Chung V, et al. High mobility group A2 potentiates genotoxic stress in part through the modulation of basal and DNA damage-dependent phosphatidylinositol 3-kinase-related protein kinase activation. Cancer Res. 2005;65:6622–6630.
26. Reeves R, Adair JE. Role of high mobility group (HMG) chromatin proteins in DNA repair. DNA Repair (Amst). 2005;4:926–938.
27. Kazmierczak B, Bullerdiek J, Pham KH, et al. Intron 3 of HMGIC is the most frequent target of chromosomal aberrations in human tumors and has been conserved basically for at least 30 million years. Cancer Genet Cytogenet. 1998;103:175–177.
28. Abe N, Watanabe T, Suzuki Y, et al. An increased high-mobility group A2 expression level is associated with malignant phenotype in pancreatic exocrine tissue. Br J Cancer. 2003;89:2104–2109.
29. Wei L, Liu X, Zhang W, et al. Overexpression and oncogenic function of HMGA2 in endometrial serous carcinogenesis. Am J Cancer Res. 2016;6:249–259.
30. Miyazawa J, Mitoro A, Kawashiri S, et al. Expression of mesenchyme-specific gene HMGA2 in squamous cell carcinomas of the oral cavity. Cancer Res. 2004;64:2024–2029.
31. Di Cello F, Hillion J, Hristov A, et al. HMGA2 participates in transformation in human lung cancer. Mol Cancer Res. 2008;6:743–750.
32. Morishita A, Zaidi MR, Mitoro A, et al. HMGA2 is a driver of tumor metastasis. Cancer Res. 2013;73:4289–4299.
33. Gao X, Dai M, Li Q, et al. HMGA2 regulates lung cancer proliferation and metastasis. Thorac Cancer. 2017;8:501–510.
34. Wang Q, Jiang S, Song A, et al. HOXD-AS1 functions as an oncogenic ceRNA to promote NSCLC cell progression by sequestering miR-147a. Onco Targets Ther. 2017;10:4753–4763.
35. Mei Y, Si J, Wang Y, et al. Long noncoding RNA GAS5 suppresses tumorigenesis by inhibiting miR-23a 5 expression in non-small cell lung cancer. Oncol Res. 2017;25:1027–1037.
36. Li X, You M, Liu YJ, et al. Reversal of the apoptotic resistance of non-small-cell lung carcinoma towards TRAIL by natural product Toosendanin. Sci Rep. 2017;7:42748.
37. Wiggins JF, Ruffino L, Kelnar K, et al. Development of a lung cancer therapeutic based on the tumor suppressor microRNA-34. Cancer Res. 2010;70:5923–5930.